

## INTERSTELLAR SCATTERING OF THE RADIO SOURCE 2013+370

STEVEN R. SPANGLER

Department of Physics and Astronomy, The University of Iowa

AND

JAMES M. CORDES

Department of Astronomy, Cornell University

Received 1987 August 20; accepted 1988 February 29

### ABSTRACT

We report the results of a six-station, 1663 MHz VLBI observation of the radio source 2013+370. The image of this source is dominated by interstellar scattering and is observed to be elliptical with a major axis (FWHM) of 17 mas and an axial ratio of 0.70. A fit of the observations to a model visibility function yields a value for  $\alpha$ , the spectral index of the power-law density irregularity spectrum, of  $\alpha = 3.79 \pm 0.05$ . Corrections for the finite angular size of the source would probably produce a *downward* revision of  $\alpha$ . Other important characteristics of the image are its smooth character, with no evidence of multiple images, and stationarity over several hours as well as over a two-year interval since a previous observation. Our observations are consistent with the interstellar density spectrum being close to Kolmogoroff for those scales which determine the angular broadening.

*Subject headings:* interferometry — interstellar medium — turbulence

### I. INTRODUCTION

Many types of radio astronomical observations reveal the presence of plasma turbulence in the interstellar medium. One of the most important characteristics of this turbulence is its spatial power spectrum. Knowledge of the spectrum can provide information on the physical mechanisms responsible for generating the turbulence, for example, via cascade from larger spatial scales as in classical fluid turbulence (Higdon 1984), or as a characteristic of compressive magnetohydrodynamic waves (Spangler *et al.* 1986; Spangler, Fey, and Cordes 1987). Furthermore, relatively large scale fluctuations in the medium can produce a variety of prominent, “refractive” scintillation effects, such as time-of-arrival variations of pulsar signals (Armstrong 1984), low-frequency variability of extragalactic radio sources and pulsars (Rickett, Coles, and Bourgois 1984), and image wandering (Lovelace 1970).

It has long been recognized that one of the most direct ways to determine the spatial spectrum is to measure the angular broadening of a radio source viewed through the turbulent medium. The interferometric visibility of a radio source is given by (Rickett 1977)

$$V(r) = \exp \left[ -\frac{D_\phi(r)}{2} \right], \quad (1)$$

where  $D_\phi$  is the phase structure function and  $r$  is the separation vector between antennas.

In this paper, we describe the results of observations intended to utilize equation (1) and obtain information on the statistical properties of density irregularities in the interstellar medium. We undertook 1663 MHz VLBI observations of the radio source 2013+370 (galactic coordinates  $l_{II} = 74.9$ ,  $b_{II} = 1.2$ ). In a previous investigation (Spangler *et al.* 1986), we found 2013+370 to manifest interstellar scattering, with an angular diameter which is optimally resolved with the United States VLBI network. These previous measurements indicated the presence of interstellar scattering because (a) the angular size of

the source at 1.67 and 0.610 GHz is considerably larger than for sources with similar spectral and variability characteristics at high latitudes and (b) the angular size between 0.610 and 5.0 GHz was observed to change as the second power of the wavelength, as expected for a scattered image. Consequently, it was considered desirable to obtain a detailed image of a source dominated by interstellar scattering in order to measure the power spectrum and isotropy of the density irregularities.

The nature of the turbulence along the line of sight to 2013+370 is uncertain. Cordes, Weisberg, and Boriakoff (1985) have argued that interstellar turbulence generally may be separated into a diffuse component with a large filling factor, and a component which is comprised of intense clumps. The scattering of 2013+370 is too large to be attributed to the diffuse component, so the observed scattering is almost certainly due to one, or a few, intense clumps along the line of sight. This object was originally observed because of its proximity to the supernova remnant G74.9+1.2. The line of sight also tranfixes the “interstellar bubble” associated with the Cygnus OB1 association. We would thus seem to have two good candidates for turbulent agitators. However, it seems that the amount of scattering observed for 2013+370 is by no means particularly large for this part of the sky (Spangler, Fey, and Mutel 1988), so it is not clear that either of these objects dominates the observed scattering. This is particularly true since the amount of scattering at low latitude seems to be much larger toward the inner galaxy. Nonetheless, whatever the astronomical association of these clumps, our observations provide information on their internal density irregularity spectrum.

### II. OBSERVATIONS AND DATA REDUCTION

The observations were carried out with elements of the United States VLBI network at a frequency of 1663 MHz, from 20 hr UT, 1986 September 29, to 5 hr UT, 1986 September 30. The interferometer consisted of antennas at Haystack, NRAO–Green Bank, North Liberty, Fort Davis, Owens Valley, and the phased VLA. Short scans of the compact sources

0106+013 and 2134+004 were included for purposes of fringe calibration. The video tapes were correlated with the new Block II correlator at the California Institute of Technology.

The correlated data were processed with a global fringe fitting algorithm in the NRAO AIPS software package. A fringe-fitting interval of 4 minutes was used. The 2 s correlator records were averaged to 30 s, after inspection revealed no discernible, systematic phase offsets. These data were edited and calibrated in the standard manner, then mapped and cleaned using the AIPS programs for these purposes. Two cycles of self-calibration were used, one with phase-only self-calibration, the second employing amplitude self-calibration. In both self-calibration cycles, a solution interval of 5 minutes was employed. Following mapping, the self-calibrated data were averaged to records of 20 minutes duration for subsequent inspection and analysis (see § IIIb below.)

The final CLEANed map is shown in Figure 1. The left panel presents the results in the form of a contour map. The right panel is a gray-scale representation of the brightness distribution. The restoring beam is 14.4 by 6.5 mas at a position angle of  $4^{\circ}.7$ . The most striking feature of the map is the smoothness of the brightness distribution. There is no evidence for clumps or structural features, despite the good quality of the map. This smoothness was also clearly evident in examination of the correlated flux density as a function of time for all baselines. Despite the heavy resolution of the source, the visibility changes in a smooth, monotonic manner, with no short time scale variations attributable to structural detail. Our interpretation of this observation is that Figure 1 is primarily showing the interstellar scattering disk rather than intrinsic structure of the source. Figure 1 also reveals an asymmetry in the source brightness distribution. The image is clearly elon-

gated, at an angle different than that of the restoring beam, as we demonstrate below.

A fit to the CLEANed map yields the following characteristics of a Gaussian model for the source brightness distribution: major axis 17 mas, minor axis 12 mas, position angle of the major axis  $12^{\circ}$ . The formal uncertainty of the fit for the position angle is less than  $1^{\circ}$ . Although we believe the true uncertainty to be somewhat larger than this, we are nonetheless confident that there is a significant difference between the position angle of the source and that of the beam. The elongated image is therefore not an artifact of the  $(u, v)$  plane coverage. In contrast to the typical situation in VLBI, a Gaussian model is not an oversimplified representation of the source brightness distribution; the functional form of the interstellar scattering disk should be quite close to Gaussian, and indeed in § III we will see that this is the case. Least-squares fits to the visibility measurements confirm the structural characteristics obtained from our map.

The observed characteristics of the source are in agreement, within the uncertainties, with the results given by Spangler *et al.* (1986) on the basis of observations made 2 yr previous to the present observations and with considerably less data. The source image therefore did not change over this 2 yr period.

### III. DISCUSSION AND INTERPRETATION

In this section we will discuss two topics, the nature of the image asymmetry and the form of the spatial spectrum of the interstellar density irregularities. For both discussions we will refer to the following power-law (spatial power) spectrum for the density fluctuations,

$$P_{\delta n}(q) = C_N^2 q^{-\alpha}, \quad q_0 \leq q \leq q_1, \quad (2)$$

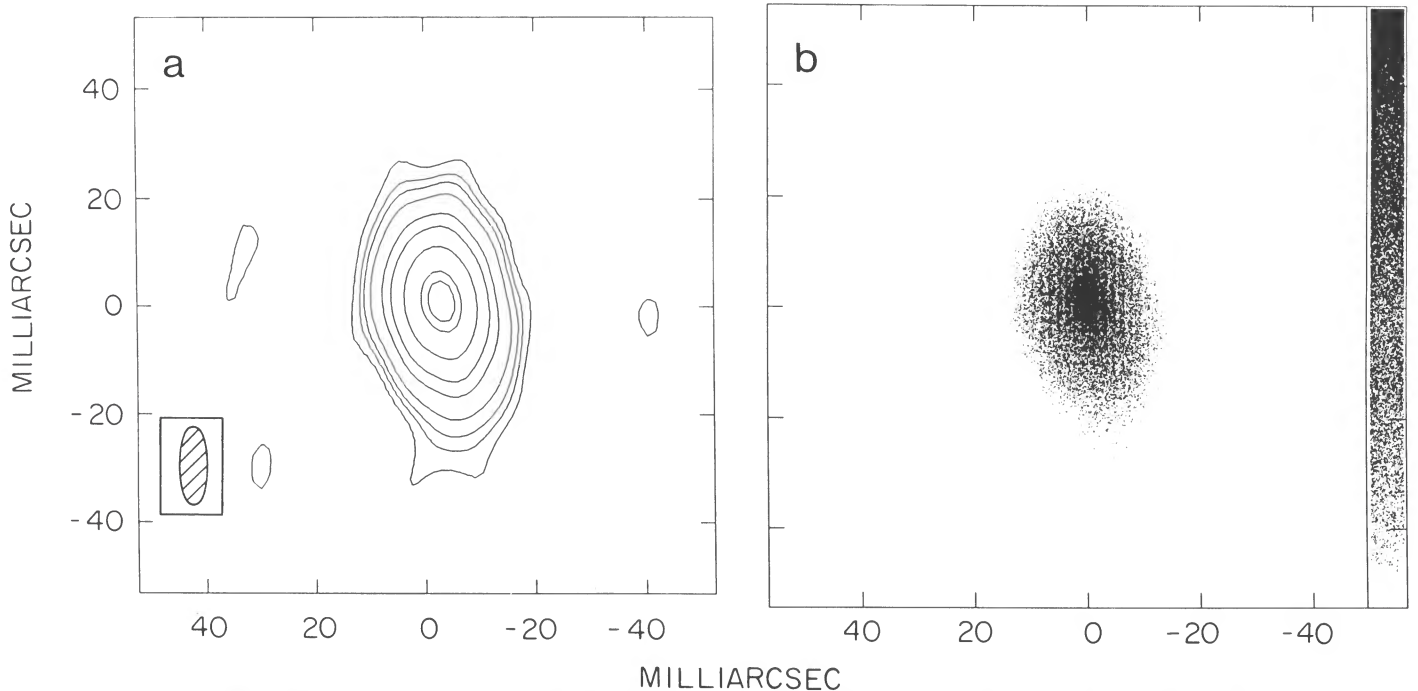


FIG. 1.—CLEANed map of the radio source 2013+370, at 1663 MHz (a) Contour plot of the source. Contours are at  $-2, 2, 4, 6, 10, 20, 30, 50, 80,$  and 90% of the peak intensity, which is 0.34 Jy per beam. The restoring beam is 14.4 by 6.5 mas, at position angle  $4^{\circ}.7$ , indicated in the box at lower left. (b) Gray-scale representation of the source brightness distribution.

defined such that the electron density variance is the three-dimensional wavenumber integral of  $P_{\delta n}(q)$ , where  $q$  is the spatial wavenumber,  $C_N^2$  is the normalization constant of the density spectrum, governing the strength of turbulence,  $\alpha$  is the power law index, and  $q_{0,1}$  are the wavenumber cutoffs for the spectrum. If  $\alpha = 11/3$ , the spectrum is referred to as "Kolmogoroff." The form of the spectrum in equation (2) assumes that irregularities are isotropic. The more general case of anisotropic irregularities is discussed below.

#### a) Image Asymmetry

We begin by discussing the asymmetry of the image, discernible in Figure 1, and revealed in the Gaussian fit described in the previous section. This asymmetry is due either to underlying intrinsic structure or an effect of the interstellar scattering.

##### i) Intrinsic Source Structure

It may be argued that Figure 1 displays an intrinsically asymmetric source which is convolved with a circularly symmetric broadening disk. Geldzahler, Shaffer, and Kühr (1984) present a 10.6 GHz map of 2013+370 which reveals an unequal double source of separation 2.1 mas at P.A.  $14^\circ$ . The position angle of this double is within a few degrees of the orientation of the major axis of the asymmetry in our image.

In spite of the coincidence of position angles, it seems improbable that the asymmetry at 1.66 GHz is due to source structure. A model for the 1.63 GHz structure of 2013+370 was made, consisting of an equal double with the same position angle and separation as revealed in the Geldzahler, Shaffer, and Kühr map. Components with equal flux densities maximize the induced asymmetry for a double model with constrained separation. The double components were chosen to be Gaussians of angular size (FWHM) 12 mas. The Gaussian structure represents the effect of isotropic interstellar scattering of each of the double components. The size of 12 mas is about the minimum necessary to reproduce our observations, which heavily resolve the source. This model was convolved with the restoring beam used in our analysis, and the model map contoured at the same levels as Figure 1. This model map (not shown) is discernibly more circular than Figure 1. To produce a synthetic map possessing the same degree of asymmetry as the observed one, the separation of the double components would have to be at least 8–10 mas, far greater than the separation observed by Geldzahler, Shaffer, and Kühr.

By way of explanation for this result, it is possible that at 1.63 GHz the intrinsic structure of 2013+370 is more extended than indicated in the 10.6 GHz map of Geldzahler, Shaffer, and Kühr. For example, perhaps the secondary component in the 10.6 GHz map is actually a knot in a jet, which becomes optically thick at lower frequencies. A weak criticism of this suggestion is that the spectrum of 2013+370 is inverted at frequencies below 10.6 GHz (Geldzahler, Shaffer, and Kühr 1984), more indicative of isolated, optically thick source components than a jet of spatially variable optical thickness, which would have a flat spectrum. Furthermore, if the intrinsic structure of 2013+370 were of the common core-jet variety, one would expect the image to display distension along the direction of the jet. In reality, the intensity along a position angle of  $12^\circ$  is quite symmetric about the position of maximum intensity. In summary, it seems unlikely that the intrinsic structure of 2013+370 is capable of producing the entire asymmetry of the 1.663 GHz image. This issue can only be resolved with a detailed VLBI image at an intermediate frequency, say 5 GHz.

##### ii) Anisotropic Interstellar Scattering

The second possibility for the observed asymmetry is that it is a property of interstellar scattering, and that the coincidence of the position angle with the intrinsic structure is fortuitous. We now consider the consequences in this case. Such an asymmetry could arise from interstellar scattering in a number of ways. First, it is possible that the irregularities themselves are anisotropic, resulting in anisotropic diffraction. This suggestion has been made by Higdon (1984, 1986) as a way of alleviating certain problems with the energetics of interstellar turbulence. Anisotropic diffraction would produce an image similar to that shown in Figure 1. Theories of wave propagation in a random medium generally assume an isotropic irregularity spectrum, given by equation (2). A simple generalization to the case of anisotropic irregularities is (Narayan and Hubbard 1988)

$$P_{\delta n}(q_x, q_y = 0) = C_N^2(\eta^2 q_x^2 + q_y^2)^{-\alpha/2}, \quad (3)$$

where  $\eta$  is a measure of the anisotropy of the irregularities. Equation (3) assumes that all scales in the medium have the same anisotropy. Although this may not be true physically, it is probably an excellent approximation since diffraction in the interstellar medium is dominated by a relatively small range of wavenumbers.

It may be shown that the axial ratio of the diffracted image is (Narayan and Hubbard 1987)

$$\frac{\theta_y}{\theta_x} = \eta. \quad (4)$$

Intuitively, this may be understood as follows. Irregularities that are longer in the  $x$ -direction are described by  $\eta > 1$ . Diffraction will therefore be less in the  $x$ -direction compared with the  $y$ -direction. If anisotropic diffraction underlies image asymmetries, then it is expected that the time scale for the image to change will be very long, since it is likely that the orientation of the irregularities is determined by large-scale structures in the medium, such as the interstellar magnetic field, or a velocity field from a stellar wind or supernova shock. This prediction is consistent with our observations.

##### iii) Anisotropic Interstellar Refraction

Another way in which scattering in the interstellar medium could produce an asymmetric image is by refractive aberration of a symmetric diffractive scattering image. This mechanism is viable if the medium produces substantially more refraction than one with  $\alpha = 11/3$  and a wavenumber cutoff  $q_1$  that is much larger than the inverse Fresnel scale,  $\sim(\lambda L)^{-1/2}$ . Such a medium might be a power law with  $\alpha > 4$  (e.g., Goodman and Narayan 1985), one with a finite cutoff  $q_1$  (Coles *et al.* 1986), or one with superposed discrete structures that are large compared with the Fresnel scale (Cordes and Wolszczan 1986; Wolszczan and Cordes 1987). There is considerable evidence favoring the presence of such discrete structures (Fiedler *et al.* 1987; Romani, Blandford, and Cordes 1987). Our discussion of refractive aberration is largely taken from the work of Cordes, Pidwerbetsky, and Lovelace (1986), who discussed refractive scattering using a thin screen mathematical model. By extrapolating their one-dimensional analysis to a two-dimensional screen, one may show that large-scale irregularities introduce a quadratic "warping" of the phase front emergent from the thin screen,

$$\phi(x, y) = a_x x + a_y y + a_{xx} x^2 + a_{yy} y^2, \quad (5)$$

where  $x$  and  $y$  are coordinates in the plane of the screen, and the coefficients  $a_x$ ,  $a_y$ , and so forth, are random functions of position. Given equation (5), it may be shown that the flux density in the absence of diffraction is given by

$$I = G_x G_y I_0, \quad (6)$$

where  $I_0$  is the flux density in the absence of such effects, and  $G_x$  and  $G_y$  are "gains," related to the warping of the phase front by

$$G_{x,y} = (1 + \lambda D a_{xx,yy}/\pi)^{-1}, \quad (7)$$

where  $D$  is the distance to the thin screen. It may be shown that, for the case of isotropic diffractive scattering with an angle  $\theta_0$ , refractive squeezing produces angular sizes of  $\theta_x = G_x \theta_0$  and  $\theta_y = G_y \theta_0$ , or an axial ratio of

$$\frac{\theta_y}{\theta_x} = \frac{G_y}{G_x}. \quad (8)$$

Values of the gains are expected to be small ( $\sim 10\%$ ) for a Kolmogoroff spectrum with  $q_1 \gg (\lambda D)^{-1/2}$ , but can approach unity if either  $q_1 \approx (\lambda D)^{-1/2}$  or if discrete structures are present. For sufficiently large  $G_{x,y}$ , however, one would expect multiple images. In summary, it is quite possible that axial ratios as large as 2 may be produced by refractive distortion of the image.

The time scale for the image to change under this process should be much shorter than that for anisotropic diffractive scattering. Here, we expect the time scale to be  $\sim t_r \approx \theta_0 D/V_\perp$ , where  $V_\perp$  is an effective transverse speed that combines motion of the irregularities and the observatory. For 2013+370, we take  $\theta_0 \approx 15$  mas,  $D = 1$  kpc, and  $V_\perp \approx 100$  km s $^{-1}$  to obtain  $t_r \approx 0.7$  yr. This is at mild variance with the observed constancy of the image over a 2 yr interval.

A final possibility for interstellar production of image asymmetry, which we think implausible, is that of multiple images, which can be produced in strong refraction. The number of images is a strong function of the underlying distribution of length scales in the medium. For media that are also diffractive, the images will be extended. If the image asymmetry of 2013+370 is caused by double imaging from an interstellar refractor, we can conclude the following.

1. The image separation must be small enough that interstellar diffraction, combined with the instrumental resolution, is sufficient to smear together the two images. In contradiction to this suggestion, we note that the image in Figure 1 is extremely smooth, with no indication of multiple images. We therefore feel this explanation can be ruled out.

2. The time scale for multiple images is more difficult to estimate, but it could be much shorter than the refractive time scale associated with a power-law irregularity spectrum. This assertion is at even worse variance with observation and furnishes a second reason for discarding multiple images as the cause of the observed asymmetry.

#### b) Electron Density Spatial Spectrum

The second issue we wish to address is a measurement of the spectral index  $\alpha$  of the density irregularities. For isotropic power law media with  $2 < \alpha < 4$ , the phase structure function is

$$D_\phi(r) \propto r^{\alpha-2}, \quad (9)$$

where  $q_1^{-1} \ll r \ll q_0^{-1}$ . A generalization to the case of aniso-

tropic scattering is considered in § IIIb(i) below. Equations (1) and (9) suggest a simple observational means of determining the index  $\alpha$ , which is to construct a plot of the logarithm of the measured visibility versus the baseline length to the power  $\alpha - 2$  for various values of  $\alpha$ . On such a plot, the data will fall on a straight line for the correct value of  $\alpha$ . A least-squares fit is used to quantify the choice of a best relationship.

The use of relation (9) in equation (1) requires that the observational measurement correspond to an ensemble average. The conditions for the measurement to converge to the ensemble average are dependent on the spectrum of density irregularities. Further discussion of this matter is given in § IIIb(iii) below, in which it will be shown that for "quasi-Kolmogoroff" spectra with  $\alpha < 4$ , conditions are satisfied for the measured visibility to correspond to the ensemble average. For the case of steep spectra with  $\alpha > 4$ , the situation is far from clear. For such spectra it is possible that measurements subject to the limitations of the technique of VLBI do not represent the ensemble average visibility.

In the strictest sense, our observations can only demonstrate consistency with  $\alpha < 4$  spectra, since it is unclear what the functional form of the visibility would be if  $\alpha > 4$ . The interpretation of angular broadening measurements would be greatly aided by a theoretical investigation of the circumstances under which observations realize the ensemble average for steep spectra, taking into account practical considerations such as the bandwidth of observation, finite fringe-fitting interval, and so on.

#### i) Fitting of the Visibility Function

To measure the spectral index  $\alpha$ , we took 20 minute averages of the source visibility, and compared the correlated flux density with the quantity  $(x^2 + \eta^{-2}y^2)^{(\alpha-2)/2}$ , hereafter referred to as the "scaled baseline." The quantities  $x$  and  $y$  are the interferometer variables  $u$  and  $v$  rotated into a frame aligned with the principal axes of the source structure. This "rotundate" baseline parameter corrects for the asymmetry of the image in the fashion of equations (3) and (4). A least-squares fit of our data yields a best value of  $\alpha = 3.79$ , with an estimated uncertainty of 0.05. In Figure 2 we present our visibility measurements versus the scaled baseline length. The solid line represents the least-squares fit of equation (1), with the phase structure function appropriate to an anisotropic,  $\alpha = 3.79$  density irregularity spectrum. In the fitting process, the data were weighted by the reciprocal of the square of the measurement error.

We examined the conformity of the data to visibility functions for other values of  $\alpha$ , using plots and fits to the data. For  $\alpha$  substantially smaller than 3.8 (i.e.,  $\alpha = 3.3$ ), the model visibility fitted the data well for medium-to-long baselines, but poorly represented the short baseline measurements, which it tended to overestimate. For  $\alpha = 4$  (the square-law structure function) on the other hand, the short and medium baselines were well described, but the observed correlated flux on long baselines is significantly higher than the model.

Finally, we undertook an additional analysis similar to that described immediately above, but in which  $\eta$  as well as  $\alpha$  was allowed to vary. The purpose of this exercise was to appraise the extent of possible uncertainty in  $\eta$  as obtained from the mapping process, and of more importance, to see if the deduced values of  $\eta$  and  $\alpha$  were correlated. For the range of  $\alpha$  considered (3.5–4.0), the  $\chi^2$  statistic showed a sharp minimum at  $\eta = 0.70 \pm 0.05$ . This preferred value showed no indication

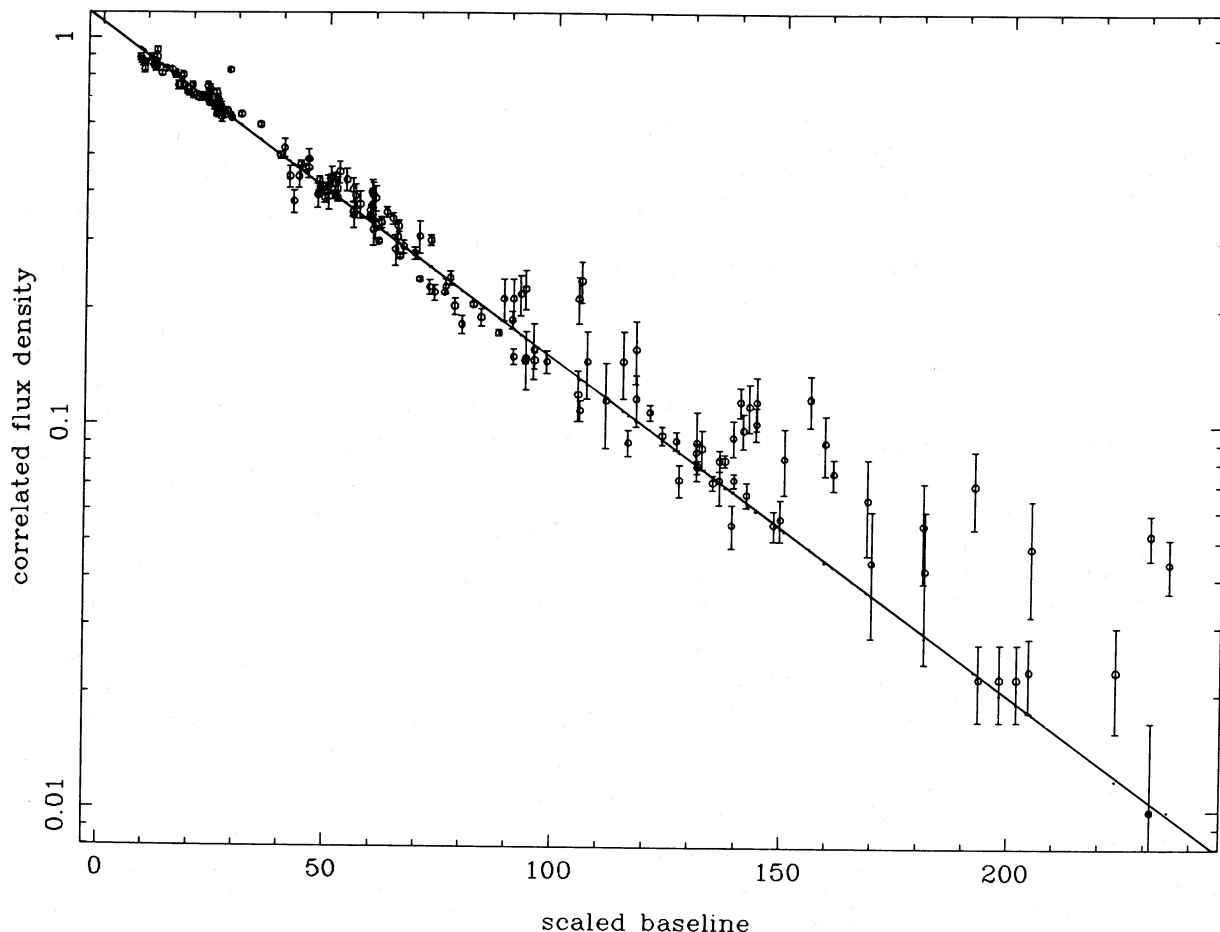


FIG. 2.—Measured visibility of the source 2013+370. The ordinate is the correlated flux density, and the abscissa is  $(x^2 + \eta^{-2}y^2)^{0.895}$ , where  $x$  and  $y$  are the interferometric variables  $u$  and  $v$  rotated into a frame aligned with the principal axes of the image. The parameter  $\eta$  is the axial ratio of the image; the parameter  $x^2 + \eta^{-2}y^2$  is therefore the square of the rotundate baseline length. Solid line represents the best fit for the visibility, given a density power spectral index of 3.79. In the fitting process, data points are weighted by the inverse square of the measurement error.

of a dependence on  $\alpha$ . Furthermore, calculations in which the position angle of the image was also allowed to change showed a pronounced increase in the computed value of the reduced  $\chi^2$ . In summary, our fitting of the visibility data confirms the main features of the source structure described in § II, and demonstrates that the uncertainties in these characteristics are both small and do not perceptibly affect the deduced value of  $\alpha$ .

#### ii) Effects of Intrinsic Source Structure

The properties of the observed visibility, enunciated in the previous paragraph, are extremely important when assessing the effect of the largely unknown intrinsic source structure on our measurements. Finite intrinsic source structure obviously tends to depress the observed visibility on long baselines more than on short baselines.

The observed visibility of a radio source affected by angular broadening is

$$V_0(r) = \exp[-\beta r^{\alpha-2} + \ln V_i(r)], \quad (10)$$

where  $\alpha$  is defined in equation (9),  $\beta$  is the appropriate normalization constant,  $r$  is the separation between the antennas (of scalar magnitude  $r$ ), and  $V_i(r)$  is the “intrinsic” visibility, i.e., that which would be observed in the absence of scattering. Equation (10) makes the simplifying assumption of isotropic scattering. For a partially resolved source, we make a Taylor’s

series expansion of  $\ln V_i(r)$ , thus generating a polynomial in  $u$  and  $v$ . The coefficients of this polynomial are determined by derivatives of the visibility, evaluated at  $r = 0$ . The derivatives of a source visibility, evaluated at zero baseline, are directly related to moments of the source brightness distribution (Thompson, Moran, and Swenson 1986, p. 320).

The implications of this result for equation (10) and our present application are as follows. For a source at the phase center, as insured by the global fringe fitting and self-calibration procedures, there will be no term linearly proportional to  $u$  or  $v$ , or to the product  $uv$ . Furthermore, for a source with a symmetric brightness distribution, the polynomial is bereft of odd powers of  $u$ ,  $v$ , and their combination. Finally, for a source which is only partially resolved, the dominant term in the expansion of  $\ln V_i(r)$  will be proportional to  $r^2$  for a circularly symmetric source, or to the square of the rotundate baseline for an elongated object. There are two requirements for the validity of this conclusion. First, the source must possess finite moments of the brightness distribution. Second, the amount of resolution must be sufficiently small as to validate truncation of the Taylor series at third order. If higher order terms in the series contribute, the intrinsic visibility may obviously not be so easily described.

Two pieces of observational evidence may be summoned to indicate that the intrinsic structure makes a small contribution

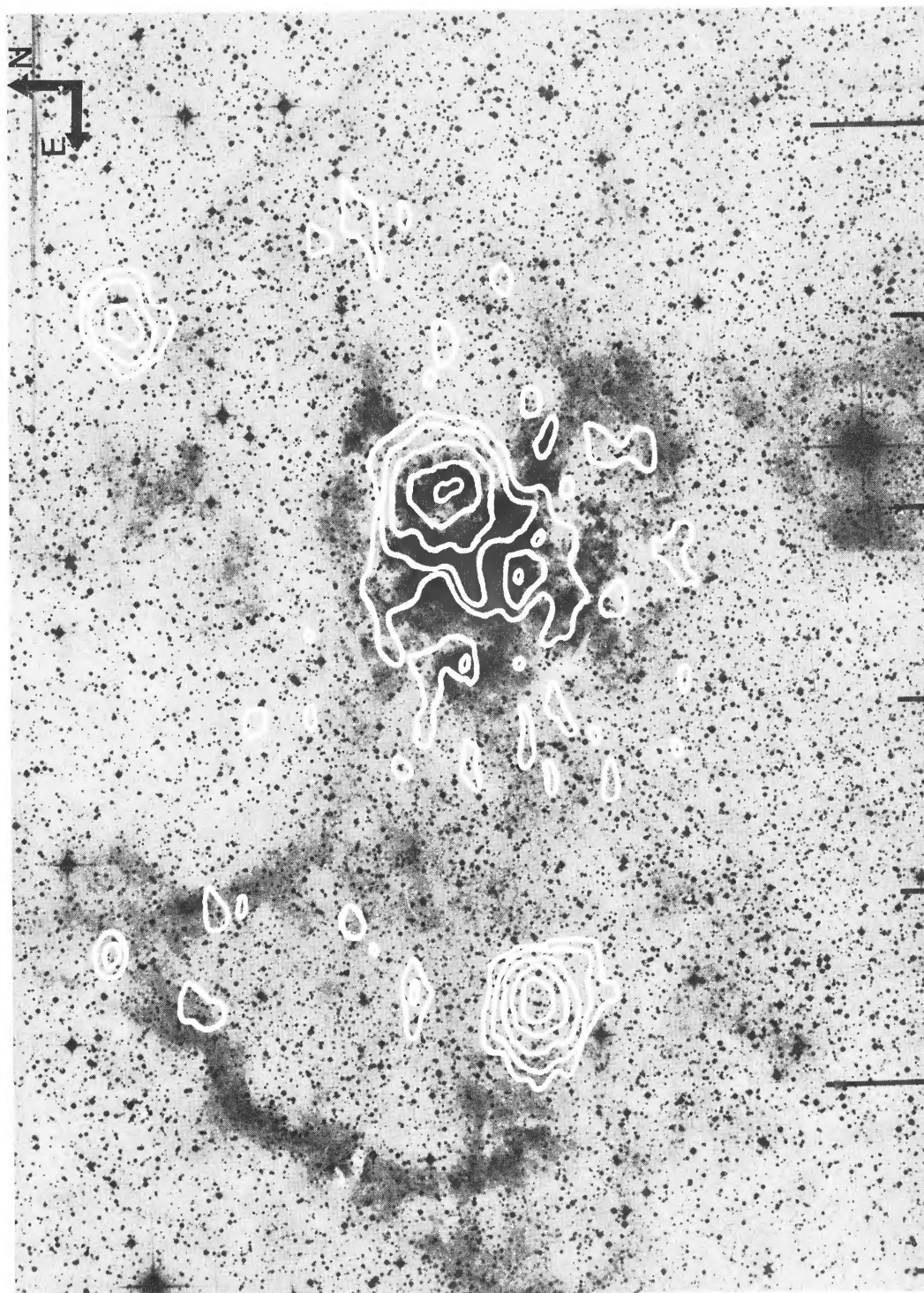


FIG. 2.—Contours of constant X-ray intensity overlaid on a red ESO sky survey plate. The isophotes are obtained from the sum of the two IPC images (I3341 and I7715) convolved with a Gaussian smoothing function of  $56''$  width (FWHM). The contour levels are at  $0.23, 0.33, 0.56, 1.12, 1.91$  counts  $\text{pixel}^{-1}$  (1 pixel =  $64 \text{ arcsec}^2$ ) corresponding to  $4 \sigma, 8 \sigma, 16 \sigma, 36 \sigma, 64 \sigma$ , over the local background.

GOLDWURM, CARAVEO, AND BIGNAMI (see 322, 350)

to the observed resolution, or in other words that  $V_i(r)$  differs little from unity, even on our longest baselines. First, our previous observations (Spangler *et al.* 1986) show the measured angular size to accurately scale as  $\lambda^2$  from 610 MHz to 5 MHz. This indicates that the scattering size dominates the intrinsic size throughout this frequency range. Second, given the structure measured by Geldzahler, Shaffer, and Kühr (1984) at 10.6 GHz, and the inverted spectrum of the source, one would expect only very slight resolution of the intrinsic structure by the interferometer used in this investigation.

The net effect of the preceding ruminations is that the second term in the argument of the exponential in equation (10) is of small magnitude and is quadratic in the baseline length. The immediately preceding data analysis procedures, resulting in Figure 2, consist in essence of fitting a single power law to these two terms. "Contamination" by the  $\ln V_i(r)$  term will thus lead to a fitted value of  $\alpha$  in excess of the true value. We therefore conclude that the best-fit value of  $\alpha = 3.79$  is probably an *overestimate* of the density spectral index  $\alpha$ . The amount by which we overestimate  $\alpha$  is again determined by the unknown source structure. Simple analyses employing reasonable estimates for the 18 cm intrinsic size of this source indicate that the correction probably is less than 0.07. The Kolmogoroff value of  $\alpha = 11/3$  is accordingly consistent with our measurements.

### iii) Effects of Image Wandering and Global Fringe Fitting

Before proceeding with further discussion, it is necessary to discuss an effect which, in principle, could influence our measurement of  $\alpha$ . The referee of this paper, William Coles, has suggested that the scattering image shown in Figure 1 *may not* strictly correspond to the Fourier transform of the ensemble average visibility, and as such may not be used to infer the spectrum of density irregularities. The spirit of Coles' argument is as follows. The scattering image corresponding to the ensemble average will in general consist of an instantaneously broadened image plus the effect of refractive wandering. Our data have been subject to global fringe fitting, with a solution interval of 4 minutes. This procedure has the effect of recentering the source at the map phase center on intervals of order 4 minutes, and thus removing the contribution of refractive wander. Most procedures for acquiring visibility data from VLBI measurements utilize closure relations, and have the same effect. An exception would be a phase reference measurement.

We now consider the influence of recentering on a scattered and refracted source. Within the context of the power law density spectra introduced in equation (2), the results will be restricted to "quasi-Kolmogoroff" spectra with  $\alpha < 4$ . However, the conclusions will more generally pertain to spectra, not necessarily of a power-law form, which produce predominantly diffractive scintillation phenomena. We consider images formed with different integration times and with different bandwidths. A snapshot image of a scattered *point* source will appear speckled, as in optical stellar images made with short exposure times. By snapshot image, we mean one that is constructed from visibilities obtained using a bandwidth and an integration time smaller than critical values of these quantities, as discussed by Cohen and Cronyn (1974). Critical values are simply the diffraction scales observed in pulsar observations (e.g., Cordes, Weisberg, and Boriakoff 1985), which are given roughly by (using parameters specific to 2013+370)

$$\begin{aligned} \Delta v_{\text{ISS}} &\approx c/D\theta_{\text{FWHM}} \approx D_{\text{kpc}}^{-1} \text{ kHz}, \\ \Delta t_{\text{ISS}} &\approx \lambda/\pi V_{\perp} \theta_{\text{FWHM}} \approx 6/V_{100} \text{ s}, \end{aligned} \quad (11)$$

where  $V_{100}$  is the perpendicular speed of scattering material in units of  $100 \text{ km s}^{-1}$ . Phase closure techniques applied to snapshot observations would place the centroid of the speckle pattern at the reference position.

It is virtually impossible to obtain such snapshot images with VLBI because sources are too weak to detect with the required bandwidth and integration time. Our phase closure time (5 minutes) and bandwidth (2 MHz) typify those used in VLBI. The speckles will be completely quenched, and the image blurred into a smooth form if the observing bandwidth  $B \gg \Delta v_{\text{ISS}}$ , integration time  $T \gg \Delta t_{\text{ISS}}$ , or source size is greater than a critical angle  $\theta_c$  given by

$$\theta_c \approx V_{\perp} \Delta t_{\text{ISS}}/D \approx 4 \times 10^{-6} \text{ mas}. \quad (12)$$

In such a case, the smoothed image will be nearly Gaussian, with a size which is the quadratic sum of the diffraction angle and intrinsic source size.

For our observations, all of these inequalities are satisfied, implying that diffraction into the angular size of  $\sim 20$  mas produces a snapshot image that is smooth, not speckled. Essentially what is happening is that a large number of independent fluctuations produced by constructive and destructive interference are averaged by the process of observing with a finite bandwidth and integration time. The number of strong maxima in a dynamic spectrum with spectral and temporal extents  $B$  and  $T$  may be conservatively estimated as

$$N \approx 10^{-2} \frac{B}{\Delta v_{\text{ISS}}} \frac{T}{\Delta t_{\text{ISS}}}, \quad (13)$$

where the numerical factor reflects the fact that the spacing of maxima is much larger than the width. For a single 5 minute integration time and  $B = 2$  MHz,  $N \approx 1000$ , and it is expected that speckles will produce visibility fluctuations of only  $N^{-1/2} \approx 3\%$ .

On longer time scales, an irregular medium generally causes wandering of the image as well as instantaneous broadening. A well-calibrated set of interferometers would yield a time-averaged image whose size reflects both wandering and scattering. Phase closure takes out wander that occurs on time scales greater than  $T$ . For a Kolmogoroff medium, wander occurs on a time scale of order

$$t_{\text{wander}} \approx D\theta_{\text{FWHM}}/V_{\perp} \approx D_{\text{kpc}}/V_{100} \text{ yr}. \quad (14)$$

Wander is less than the observed *instantaneous* angular size (Cordes, Pidwerbetsky, and Lovelace 1986), and has an amplitude that increases linearly with time for time scales longer than  $\Delta t_{\text{ISS}}$ . Thus, the amount of wander occurring on the time scale  $T$  (5 minutes) is completely negligible. Consequently, for a Kolmogoroff medium, we assume that phase closure causes negligible distortion of the image and the calibrated visibilities may be used to constrain the wavenumber spectrum, as we have done.

It has been argued (Coles *et al.* 1986) that the inner scale may be comparable to the Fresnel scale, or  $q_1(\lambda D)^{1/2} \approx 1$ , in order to explain intensity variations that are refractive in origin. We refer to this case as a modified Kolmogoroff medium if the slope of the wavenumber spectrum is  $11/3$ . For this case, the snapshot image would consist of several to many single images, depending on the strength of scattering. The number of sub-images contributing to a snapshot image of 2013+370 is roughly

$$N_i \approx \frac{(D\theta_{\text{FWHM}})^2}{\lambda D} \approx 10^{6.2} D_{\text{kpc}}. \quad (15)$$

Thus, although image fluctuations are expected to occur on a time scale

$$t_i \approx (\lambda D)^{1/2} / V_{\perp} \approx 7 / V_{100} \text{ hr}, \quad (16)$$

the amount of fluctuation is only  $1/(N_i)^{1/2} \approx 0.1\%$ .

Finally, we consider the case of a steep power law, i.e.,  $\alpha > 4$ , for which the snapshot image is volatile in structure on both large and small time scales. The minimum time scale for change is roughly  $t_i \approx 7/V_{100}$  hr, but the largest variations (which we assume to be of order the size of the instantaneous image) would occur on a much longer time scale of

$$t_{\text{long}} \approx D\theta_{\text{FWHM}}/V_{\perp} \approx D_{\text{kpc}}/V_{100} \text{ yr}.$$

The image would contain structure on many scales, although the smallest ones would be washed out given the bandwidth and integration time of our data. We have argued before that such an image is completely inconsistent with our results: the image is well modeled as an elliptical Gaussian function.

In addition to the above theoretical considerations, a number of circumstantial observational arguments may be mustered to indicate that “refractive wandering” is not an important phenomenon in the case of 2013+370, and that the image shown in Figure 1 represents a robust, stationary measurement of the interstellar scattering disk. These arguments are predicated on an assumption regarding the way in which refractive effects would manifest themselves in interferometric measurements. The true state of affairs for interstellar scattering is at present unknown. We assume that the effect of refraction would be to produce detectable distortion of the diffractive image in addition to refractive image wandering. This assumed distortion, which might take the form of image elongation or subimage formation, would change on the time scale discussed in § IIIa(iii).

In Spangler *et al.* (1986), we showed that the measured angular size of 2013+370 scales accurately as  $\lambda^2$ . If refractive wandering were important, our measurements would have been malformed, poor realizations of the scattering process, and one might not expect the  $\lambda^2$  scaling.

Furthermore, as noted in § II, the scattering image obtained here is in good agreement with one obtained 2 yr previously. This indicates that a robust measurement was made in both observing sessions, that the image shown in Figure 1 is stationary over periods of at least 2 yr, and refractive wandering contributes little to the scattering image of this source.

A final test of a similar nature was carried out on the data from the present observations. Our correlator data were in two blocks, the first containing observations from the first 6 hr of the session, and the second containing the last 3 hr. If refractive wandering were an important contributor to the scattering image, the image should depend on the duration of the observing program. Accordingly, one would expect maps emergent from the data subsets to disagree both with each other and with the map generated from the entire data set. On the other hand, if the map in Figure 1 is a robust estimate of the scattering function, then images created from subsets of the data should be in agreement with each other and the integral map, given allowance for estimation error due to the poorer ( $u, v$ ) plane coverage of the data subsets.

Maps generated from these data subsets did indeed show satisfactory agreement with the integral map regarding major axis, axial ratio, and position angle. We believe these arguments indicate that our observations represent a good estimate

of the ensemble average scattering function and may be interpreted accordingly.

In summary, we believe that although phase closure techniques generally remove image wandering that occurs on time scales longer than the integration time, the amount of wander produced by the interstellar medium on such time scales is negligible. The image we have obtained using global fringe fitting and self-calibration is therefore an accurate representation of the scattering produced by the interstellar medium.

#### iv) Other Recent Constraints on $\alpha$

It is interesting to note that independent and very recent observational results support our conclusions. Wilkinson, Spencer, and Nelson (1988) have analyzed angular broadening measurements of the radio source Cygnus X-3, and deduce a value of  $\alpha = 3.85 \pm 0.05$ . Gwinn *et al.* (1988) report preliminary results of a search for differential position fluctuations in  $\text{H}_2\text{O}$  maser sources. Restrictive limits on such fluctuations were obtained. While the data of Gwinn *et al.* do not permit a precise determination of  $\alpha$ , they exclude values of  $\alpha$  greater than 3.9 subject to caveats related to values of the wavenumber cutoffs  $q_0$  and  $q_1$  (see eq. [2]).

It is worth noting that a variety of effects can result in an inferred value of  $\alpha$  greater than four: actual power-law spectra with  $\alpha > 4$ , power-law spectra with  $\alpha < 4$  but possessing an inner scale cutoff comparable to the Fresnel scale, or power-law spectra with  $\alpha < 4$  augmented by large-scale, possibly non-turbulent, refractive “prisms” (Coles *et al.* 1987). Our observational result suggests that none of these is dominant in the turbulence along the line of sight to 2013+370.

These preceding observational studies, consistent with an interstellar density irregularity power spectrum close to the Kolmogoroff value, raise an interesting dilemma with respect to the interpretation of other observations. Several radioastronomical phenomena, such as prominent band structures in pulsar dynamic spectra (Cordes and Wolszczan 1986; Wolszczan and Cordes 1987), strong refraction effects in flux density time series of extragalactic radio sources (Fiedler *et al.* 1987), and perhaps low-frequency variability (Rickett, Coles, and Bourgois 1984), have been attributed to propagation through a medium with a steep density irregularity power spectrum. The magnitude of these effects would be greatly diminished, to a degree incompatible with observation, if the intervening interstellar medium has a Kolmogoroff density spectrum with negligible inner scale.

How then are we to resolve this situation in which such dissimilar conclusions about interstellar turbulence emerge from different types of observations? In response, we note that the strength of scattering is generally quite different for the two types of phenomena. Refractive effects have generally been observed for nearby pulsars or high-latitude extragalactic sources. Our observations, as well as those of Wilkinson, Spencer, and Nelson (1988) and Gwinn *et al.* (1988) are of highly scattered objects, whose lines of sight traverse a large distance through the interstellar medium. It has been previously noted by Cordes, Weisberg, and Boriakoff (1985), that highly scattered lines of sight are probably dominated by a few intense clumps of turbulence, termed the “type B” medium by those authors. For weakly scattered objects, on the other hand, we are seeing the effect of a diffuse, distributed turbulence, referred to by Cordes, Weisberg, and Boriakoff as “type A” turbulence. It might therefore be conjectured that the intense

clumps sampled by our observations are characterized by a relatively shallow (i.e.,  $\alpha < 4$ ) density power spectrum, whereas the diffuse medium either has a steeper power law or a Kolmogoroff-like power law with additional structure at high or low wavenumbers. Alternatively, the turbulence might be similar in both media, consisting of Kolmogoroff turbulence with appended, large-scale "lens." For high-latitude lines of sight or nearby pulsars, refractive effects due to these lens would dominate, whereas for highly scattered lines of sight the refractive effects would average out and diffractive effects due to the Kolmogoroff component would be most pronounced. Indeed, the scattering disk size of 2013+370 is  $D\theta_{\text{FWHM}} \approx 20D_{\text{kpc}}$  astronomical units, possibly much larger than the sizes of lens required for pulsar refraction events.

In entertaining these notions, it is necessary to keep in mind the observations of Dennison *et al.* (1987), who have identified flux density variations of 2013+370 which they associate with refractive scintillations. While refractive scintillations are generally thought of as a manifestation of steep ( $\alpha > 4$ ) irregularity spectra, the amplitude of the 2.7 GHz fluctuations discussed by Dennison *et al.* (1987) was rather small, of the order 5%. It seems quite plausible that the irregularity spectrum deduced from our observations is capable of producing scintillations of this magnitude.

#### IV. CONCLUSIONS

The 1663 MHz VLBI image of 2013+370 has been analyzed to deduce properties of interstellar turbulence along the line of sight. A least-squares fit to the measured visibilities yields a value of  $\alpha = 3.79 \pm 0.05$ , where  $\alpha$  is the index of the power-law density irregularity spectrum. This value does not include any correction for the poorly known intrinsic structure. The effect of corrections for intrinsic structure would most probably be to revise  $\alpha$  downward. Our measurements are therefore consistent with the density turbulence along the line of sight to this object having a spectrum similar to the Kolmogoroff one.

Also consistent with a "quasi-Kolmogoroff" spectrum are the smoothness of the image, with no evidence of multiple components, and its stability over a 2 yr period. The observed asymmetry of the observed image is probably due either to underlying intrinsic structure or anisotropic irregularities.

This research was supported at the University of Iowa by grants NAGW-806 and NAGW-831 from the National Aeronautics and Space Administration. At Cornell University, we were supported by the Alfred P. Sloan Foundation, NSF grant AST-8520530, and the National Astronomy and Ionosphere Center. The authors thank Alan Fey of the University of Iowa for overseeing the correlation of the data tapes.

#### REFERENCES

- Armstrong, J. W. 1984, *Nature*, **307**, 527.  
 Cohen, M. H., and Cronyn, W. M. 1974, *Ap. J.*, **192**, 193.  
 Coles, W. A., Frehlich, R. G., Rickett, B. J., and Codona, J. L. 1986, *Ap. J.*, **315**, 666.  
 Cordes, J. M., Pidwerbetsky, A., and Lovelace, R. V. E. 1986, *Ap. J.*, **310**, 737.  
 Cordes, J. M., Weisberg, J. M., and Boriakoff, V. 1985, *Ap. J.*, **288**, 221.  
 Cordes, J. M., and Wolszczan, A. 1986, *Ap. J. (Letters)*, **307**, L27.  
 Dennison, B., *et al.* 1987, *Ap. J.*, **313**, 141.  
 Fiedler, R., *et al.* 1987, *Nature*, **326**, 375.  
 Geldzahler, B. J., Shaffer, S. B., and Kühr, H. 1984, *Ap. J.*, **286**, 284.  
 Goodman, J., and Narayan, R. 1985, *M.N.R.A.S.*, **214**, 519.  
 Gwinn, C. R., Moran, J. M., Reid, M. J., and Schnepps, 1988, in *IAU Symposium 129, The Impact of VLBI on Astrophysics and Geophysics* ed. M. J. Reid and J. M. Moran (Dordrecht: Reidel), p. 295.  
 Higdon, J. C. 1984, *Ap. J.*, **285**, 109.  
 ———. 1986, *Ap. J.*, **309**, 342.  
 Lovelace, R. V. E. 1970, Ph.D. thesis, Cornell University.  
 Narayan, R., and Hubbard, W. B. 1988, *Ap. J.*, **325**, 503.  
 Rickett, B. J. 1977, *Ann. Rev. Astr. Ap.*, **15**, 479.  
 Rickett, B. J., Coles, W. A., and Bourgois, G. 1984, *Astr. Ap.*, **134**, 390.  
 Romani, R. W., Blandford, R. D., and Cordes, J. M. 1988, *Ap. J.*, submitted.  
 Spangler, S. R., Fey, A. L., and Cordes, J. M. 1987, *Ap. J.*, **322**, 909.  
 Spangler, S. R., Fey, A. L., and Mutel, R. L. 1988, in *IAU Symposium 129, The Impact of VLBI on Astrophysics and Geophysics* (Dordrecht: Reidel), p. 303.  
 Spangler, S. R., Mutel, R. L., Benson, J. M., and Cordes, J. M. 1986, *Ap. J.*, **301**, 312.  
 Thompson, A. R., Moran, J. M., and Swenson, G. W., Jr. 1986, *Interferometry and Synthesis in Radio Astronomy* (New York: Wiley).  
 Wilkinson, P. N., Spencer, R. E., and Nelson, R. F. 1988, in *IAU Symposium 129, The Impact of VLBI on Astrophysics and Geophysics* ed. M. J. Reid and J. M. Moran (Dordrecht: Reidel), p. 305.  
 Wolszczan, A., and Cordes, J. M. 1987, *Ap. J. (Letters)*, **320**, L35.

JAMES M. CORDES: Department of Astronomy, Cornell University, Ithaca, NY 14853

STEVEN R. SPANGLER: Department of Physics and Astronomy, The University of Iowa, Iowa City, IA 52242